JVI Accepts, published online ahead of print on 16 July 2014
J. Virol. doi:10.1128/JVI.01582-14

Seed-sequence matched controls reveal limitations of siRNA knockdown in functional and structural studies of HCV NS5A-MOBKL1B interaction

Hyo-Young Chung[1], Meigang Gu[1], Eugen Buehler[2], Margaret R. MacDonald[1], and Charles M. Rice[1, #]

[1]Center for the Study of Hepatitis C, Laboratory of Virology and Infectious Disease, The Rockefeller University, New York, NY 10065, USA

[2]Division of Preclinical Innovation, National Center for Advancing Translational Sciences, National Institutes of Health, Bethesda, MD 20892, USA

Running title: The pitfalls of siRNA: a case study with HCV NS5A

#Correspondence and requests for materials should be addressed to C.M.R. (e-mail: ricec@mail.rockefeller.edu).

Abstract word count: 247

Importance word count: 142

Manuscript text word count: 6 490

Abstract

Hepatitis C virus (HCV) is a widespread human pathogen causing liver cirrhosis and cancer. Similar to other viruses, HCV depends on host and viral factors to complete its life cycle. We used proteomic and yeast two-hybrid approaches to elucidate host factors involved in HCV nonstructural protein NS5A function and found that MOBKL1B interacts with NS5A. Initial experiments with siRNA knockdown suggesting a role in HCV replication led us to examine the interaction using biochemical and structural approaches. As revealed by a co-crystal structure of a core MOBKL1B–NS5A peptide complex at 1.95 Å, NS5A binds to a hydrophobic patch on the MOBKL1B surface. Biosensor binding assays identified a highly conserved, 18 amino acid binding site in domain II of NS5A, which encompasses residues implicated in cyclophilin A (CypA)-dependent HCV RNA replication. However, a CypA-independent HCV variant had reduced replication in MOBKL1B knockdown cells, even though its NS5A does not interact with MOBKL1B. These discordant results prompted more extensive studies of MOBKL1B gene knockdowns, which included additional siRNAs and specifically matched seed-sequence siRNA controls. We found that reduced virus replication after treating cells with MOBKL1B siRNA was actually due to off-target inhibition, and indicated that the initial finding of virus replication dependence on the MOBKL1B-NS5A interaction was incorrect. Ultimately, using several approaches we found no relationship of the MOBKL1B-NS5A interaction to virus replication. These findings collectively serve as a reminder to investigators and scientific

reviewers of the pervasive impact of siRNA off-target effects on interpretation of biological data.

Importance

Our study illustrates an underappreciated shortcoming of siRNA gene knockdown technology. We initially identified a cellular protein, MOBKL1B, as a binding partner with the NS5A protein of hepatitis C virus (HCV). MOBKL1B siRNA, but not irrelevant RNA treatment was associated with both reduced virus replication and the absence of MOBKL1B. Believing that HCV replication depended on the MOBKL1B-NS5A interaction, we carried out structural and biochemical analyses. Unexpectedly, an HCV variant lacking the MOBKL1B-NS5A interaction could not replicate after cells were treated with MOBKL1B siRNA. By repeating the MOBKL1B siRNA knockdowns, and including seed sequence-matched siRNA instead of irrelevant siRNA as a control, we found that the MOBKL1B siRNAs utilized had off-target inhibitory effects on virus replication. Collectively, our results suggest that stricter controls must be utilized in all RNAi-mediated gene knockdown experiments to ensure sound conclusions and a reliable scientific knowledge database.

Introduction

Hepatitis C virus (HCV) is an enveloped RNA virus in the *Flaviviridae* family, in which there are seven major genotypes diverging by 30-35% at the nucleotide level. Globally, more than 170 million people are infected by HCV, and although 20-30% of acute HCV infections are spontaneously cleared, the majority of virus-exposed individuals develop chronic infection, which can lead to liver cirrhosis, end-stage liver disease and hepatocellular carcinoma (1). Despite new treatment options that are highly effective (2), drug resistance and incomplete genotype coverage are important limitations. Thus, it is important to thoroughly understand the mechanistic activity of inhibitors, and to develop additional antivirals directed at different targets.

The HCV genome is a ~9.6 kb positive-sense single-stranded RNA encoding a single open reading frame, which is translated into a polyprotein precursor. From the polyprotein, three structural proteins (core, envelope proteins E1 and E2) and seven nonstructural proteins (p7, NS2, NS3, NS4A, NS4B, NS5A and NS5B) are produced after a series of co- and post-translational cleavages by both host and viral proteases. The genome is replicated in an altered intracellular membrane-associated replication complex that is composed of viral and cellular factors [reviewed in (3)].

Along with other HCV proteins, NS5A has been the focus of intensive inhibitor discovery efforts, and highly potent new compounds targeting it have been shown to be clinically efficacious (4). NS5A is a phosphoprotein with multiple roles in the virus life cycle, including virus genome replication and

particle assembly (5–7). However, the mechanistic activity of HCV NS5A is not fully understood. In an effort to broaden our understanding of NS5A, our objective was to define its interaction with cellular partners. To this end, we performed a pull-down assay of Huh-7.5 hepatoma cells infected with a genotype 2a virus expressing a tagged NS5A, and discovered a novel NS5A-interacting protein, Mps one binder kinase activator-like 1B (MOBKL1B, also termed MOB1A). MOBKL1B is a component of the protein kinase cascade of the Salvador/Warts/Hippo (SWH) tumor suppressor pathway, and although it has no known enzymatic activity, it plays an important role in the pathway as an activator of nuclear Dbf2-related (NDR) serine/threonine kinases (8–10).

To test whether the NS5A-MOBKL1B binding was functionally significant for HCV replication we took a typical approach and performed MOBKL1B siRNA knockdown experiments in permissive hepatoma cells before infection. Results from these initial studies indicated that virus replication required MOBKL1B expression, prompting us to characterize the NS5A-MOBKL1B with biochemical, genetic, and structural studies. We showed that the MOBKL1B-binding site on NS5A overlapped with the binding site of cyclophilin A (CypA), a cellular protein that is essential for HCV RNA replication, as its interaction with NS5A enhances HCV RNA binding (11–14). CypA has emerged as the first host factor targeted for anti-HCV therapy, and drugs blocking the CypA–NS5A interaction are currently in various stages of clinical development (15). Mutant HCVs that replicate in the absence of CypA have amino acid substitutions in the CypA binding site of NS5A, and because of the overlap of MOBKL1B and CypA binding

sites, we questioned whether these mutations would also affect NS5A-MOBKL1B interactions. With protein pull-down experiments, we found that a CypA-independent mutant NS5A did not interact with MOBKL1B. However, the CypA-independent virus had reduced replication after cells were treated with MOBKL1B siRNA, which was unanticipated, since a virus lacking the MOBKL1B-NS5A interaction would not be expected to depend on it for replication. This contradiction prompted us to re-examine our MOBKL1B siRNA gene knockdown experiments with wild-type HCV. After including matched seed-sequence controls alongside our siRNAs targeting MOBKL1B, we showed off-target inhibitory effects of siRNA treatment on virus replication. Our cumulative results ultimately showed that HCV replication in cultured cells does not depend on an interaction between MOBKL1B and NS5A. We conclude that for accurate interpretation, gene knockdowns should be performed with multiple siRNAs with stringent matched controls, rather than the more commonly used irrelevant or non-silencing siRNA controls.

Materials and Methods

Cells and antibodies

Huh-7.5 cells were maintained in DMEM containing 10% fetal bovine serum (FBS) and 0.1 mM nonessential amino acids (NEAA) at 37°C in a 5% CO_2 incubator. Rabbit polyclonal antibody against MOBKL1B was purchased from Cell Signaling Technology (Danvers, MA). Mouse anti-CypA antibody was purchased from Santa Cruz Biotechnology (Santa Cruz, CA), and mouse anti-NS3 antibody (H23) was from Abcam (Cambridge, United Kingdom). The mouse anti-NS5A antibody 9E10 has been previously described (16).

Plasmid construction

Affinity-tagged Jc1 constructs for the pull-down experiment. The One-STrEP-tag (OST, IBA GmbH, Gottingen, Germany) was introduced into the Jc1 genome (17) at a position between NS5A residues 383 and 384, which was previously shown to be tolerant to tag insertion (18) to generate Jc1 NS5A-OST. The D316E Y317N (DEYN) CypA-independent mutant virus, termed Jc1 NS5A-OST-DEYN was constructed using the megaprimer overlapping PCR method. This strategy was also used to introduce the DEYN mutations into Jc1 FLAG (p7-nsGluc2A) (19) to construct Jc1 FLAG (p7-nsGluc2A) DEYN.

Yeast two-hybrid constructs. MOBKL1B cDNA (GenBank: BC003398) was amplified and cloned into pGADT7 (activation domain) vector (Clontech, Mountain View, CA) using 5' *Nde*I and 3' *BamH*I cloning sites. Genes encoding each viral protein were amplified from Jc1 or Con1 (7) genome-containing

plasmids and cloned into pGBKT7 (binding domain) vector (Clontech) using 5' *Nde*I/3' *BamH*I or 5' *EcoR*I/3' *BamH*I cloning sites. Con1 NS5A domain II serial deletion mutants were subcloned using the genotype 1b HCV replicon (7) and JFH1 NS5A alanine substitution mutants were constructed using the megaprimer method.

MOBKL1B bacterial expression constructs. MOBKL1B cDNA was amplified with primers containing 5' *BamH*I and 3' *Xho*I restriction sites and cloned into pET-SUMO vector (Invitrogen, Carlsbad, CA).

GST fused NS5A peptide constructs. 5' phosphorylated sense and antisense oligonucleotides encoding NS5A residues 310–335, 310–327, 310–324, 310–320, 314–329, 305–316 and 308–327 were synthesized with 5'-*EcoR*I/3'-*Not*I linkers (IDT, Coralville, IA). Oligonucleotides were annealed and cloned into pGEX-6P-1 vector (GE Healthcare, Uppsala, Sweden) using 5'-*EcoR*I/3'-*Not*I cloning sites.

Protein pull-down and mass spectrometry identification

To identify cellular proteins interacting with viral proteins, *in vitro* transcribed Jc1 NS5A-OST RNA was electroporated into Huh-7.5 cells (10 plates of 150 mm dishes) as described previously (20). Cells were harvested 72 h post-electroporation by incubation in 1 ml of lysis buffer (LB: 20 mM Tris, pH 8.0, 150 mM NaCl, 2 mM $MgCl_2$ and 1% Triton X-100) supplemented with EDTA-free protease inhibitor cocktail (Roche, Basel, Switzerland), DNase I (50 U/ml) and RNase A (10 µg/ml). Lysates were clarified by centrifugation (16,000 x *g*, 20 min,

4°C) and incubated with 50 µl of Strep-Tactin Sepharose (IBA GmbH, Gottingen, Germany) for 2 h at 4°C. The matrix was washed 5 times in LB. Bound proteins were released by boiling in SDS-PAGE loading buffer, separated by 4–20% SDS-PAGE, and visualized by Coomassie staining. Proteins in SDS-PAGE were digested with trypsin, extracted and identified by liquid chromatography with online tandem mass spectrometry (LC-MS/MS). Peptide mass fingerprinting analysis was performed using Mascot Search (Matrix Science, Boston, MA) against the SwissProt database (downloaded Aug, 2008).

RNA interference

siRNAs corresponding to MOBKL1B coding nt 241–259 (#1, 5'-GAAGCAAGCUGUCCAGUCA-3'), nt 91–111 (#2, 5'-CAUGCAGAAGCAACUCUAGGA-3') or nt 292–310 (#3, 5'-GCAGAUGGUACUAAUAUUA-3'), their seed-sequence matched siRNA controls (#1 C911, 5'-GAAGCAAGGACUCCAGUCA-3'; #2 C1012, 5'-CAUGCAGAACGUACUCUAGGA-3'; #3 C911, 5'-GCAGAUGGAUGUAAUAUUA-3') and pools of MOBKL1B, CypA targeting siRNAs (ON-TARGETplus SMARTpools) and irrelevant siRNA designed for minimal targeting of human genes (ON-TARGETplus Non-Targeting Pool) were purchased from Dharmacon (Lafayette, CO). For the depletion of target proteins, ~3.0 x 10^4 Huh-7.5 cells per well were seeded in 24-well plates 1 d before transfection. Cells were transfected twice in 24 h intervals with 50 nM siRNA using 1.5 µl of Lipofectamine™ RNAiMAX following the manufacturer's

196 instructions (Invitrogen).

197

198 **HCV replication and production assays**

199 HCV Jc1 virus stock was generated by electroporation of Huh-7.5 cells
200 with *in vitro* transcribed RNA as previously described (20), and its infectious titer
201 was determined by limiting dilution assay followed by NS5A staining (16). To
202 initiate infection with RNA, wild type or the DEYN mutant Jc1FLAG(p7-nsGluc2A)
203 plasmid was linearized by *Xba*I digestion and RNA was generated by *in vitro*
204 transcription using the T7 RiboMAX transcription kit following the manufacturer's
205 instructions (Promega, Madison, WI). Viral RNAs (500 ng per well of a 24 well
206 plate) were transfected into Huh-7.5 cells in DMEM supplemented with 1% FBS
207 and 0.1 mM NEAA using 1 µl of Lipofectamine2000 (Invitrogen). Plates were
208 centrifuged at 1,000 x *g* for 30 min at 37ºC. Media were replaced 6 h later with
209 DMEM containing 10% FBS and 0.1 mM NEAA. Viral RNA replication was
210 assayed by measuring luciferase released into the medium over time (at 6, 24,
211 48 and 72 h post-transfection) using the *Renilla* Luciferase Assay System
212 (Promega).

213 To analyze infectious virus production from HCV Jc1FLAG(p7-nsGluc2A),
214 naïve Huh-7.5 cells were incubated with cell culture supernatant containing
215 infectious virus for 4 h and exchanged with fresh media. Luciferase detection in
216 the supernatant was carried out 2 d after infection by *Renilla* Luciferase Assay
217 System (Promega).

218 J6/JFH-1 based NS5A recombinant virus (21) was produced by

transfecting *in vitro* transcribed RNA into Huh-7.5 cells, followed by determination of infectious titer by limiting dilution assay staining for NS3.

Western blotting

Cells were lysed in PBS containing 1% Triton X-100, 0.05% SDS, 0.5% deoxycholate and EDTA-free protease inhibitor cocktail (Roche) for 10 min on ice. Lysates were clarified by centrifugation (16,000 x*g*, 10 min, 4°C) and proteins were separated on 4–12% SDS-PAGE gels. Proteins were transferred onto polyvinylidene difluoride membrane (Millipore, Billerica, MA). Blots were incubated with primary antibodies against MOBKL1B (1:1,000; Cell Signaling Technology), CypA (1:1,000; Santa Cruz Biotechnology) or β-actin (1:10,000; Sigma), followed by horseradish peroxidase-conjugated goat anti-rabbit or goat anti-mouse secondary antibody (1:10,000; Jackson ImmunoResearch, West Grove, PA). Proteins were detected using Super Signal West Pico substrate (Thermo Scientific, Waltham, MA).

Cytotoxicity assay

Toxicity of the MOBKL1B knockdown was evaluated using the CellTiter-Glo® Luminescent Cell Viability assay following the manufacturer's instructions (Promega). Huh-7.5 cells were transfected twice at 24 h intervals with three individual MOBKL1B-specific siRNAs (#1, #2 and #3), their mismatch siRNAs (#1 C911, #2 C1012 and #3 C911) or irrelevant (IRR) siRNA. Cells were lysed in CellTiter-Glo® reagent 48 h after the second siRNA transfection and assessed for

the luminescent signal.

Yeast two-hybrid binding assays

Yeast two-hybrid binding assays were performed as described previously (22) using the Matchmaker GAL4 Yeast Two Hybrid 3 system (Clontech).

Purification of recombinant proteins

Full-length MOBKL1B and MOBKL1B$_{33–216}$ were expressed as His$_6$-Smt3 N- terminal fusion proteins in Rosetta (DE3) cells (Merck KGaA, Darmstadt, Germany). The cells were grown to reach A_{600} ~ 0.8 and induced for the protein expression with 0.5 mM IPTG. After incubation for 5 h at 25ºC, cells were harvested by centrifugation and lysed for 30 min at 4ºC using a lysis buffer consisting of 20 mM Tris, pH 8.0, 50 mM imidazole, 500 mM NaCl and EDTA-free protease inhibitor cocktail (Roche) containing 10 mg/ml lysozyme, followed by sonication. Lysates were clarified by centrifugation (35,000 x *g*, 30 min, 4°C) and passed through a Ni-Sepharose 6 Fast Flow (GE Healthcare, Uppsala, Sweden) column. Unbound and nonspecifically bound materials were washed off using wash buffer (20 mM Tris, pH 8.0, 50 mM imidazole and 25 mM NaCl) and bound proteins were eluted with the same buffer containing 250 mM imidazole. The His$_6$-Smt3 tag was removed as described (23) from eluted proteins by incubation with Ulp1 protease (100 µg/10 mg protein, 4 h, 4°C). The proteins were further purified by ion-exchange chromatography (HiTrap Q HP, GE Healthcare), a second pass over Ni-Sepharose 6 Fast Flow to remove free His$_6$-

Smt3 tag, and finally size exclusion chromatography (Superdex 75, GE healthcare) in buffer containing 20 mM Tris, pH 7.5, 50 mM NaCl, 2 mM DTT and 10% glycerol. MOBKL1B proteins were concentrated to 25 mg/ml using Amicon Ultra-15 Centrifugal Filter Unit (Millipore).

Biosensor analyses

Biosensor binding experiments were performed using BIACORE2000 (GE Healthcare) and ForteBio Octet Red 384 (ForteBio, Menlo Park, CA) instruments. For the experiments using the BIACORE2000 instrument, ~ 5,000 RU (response units) of anti-GST antibody was immobilized on flow cells of the research-grade CM5 sensor chip using amine-coupling chemistry (24). GST-NS5A peptides or GST alone were captured from soluble *E. coli* lysates on the antibody surface at densities of 1.5 ~ 2.5 kRU. Pure full-length MOBKL1B protein at the designated concentrations was injected in triplicate in running buffer (20 mM sodium phosphate, pH 7.2, 150 mM NaCl, 0.1 mg/ml BSA and 0.01% Tween-20) at a flow rate of 50 µl/min at 25ºC. Data were collected at a rate of 2 Hz during 50 sec association and dissociation phases. All interactions reached equilibrium rapidly and dissociated completely within seconds. Equilibration constants were obtained by fitting the responses at 25 sec to a simple one-to-one binding interaction isotherm (25). The experiments using ForteBio Octet Red 384 were performed as described above, except that the running temperature was 30ºC.

Crystallization

Termini-blocked (N, acetyl; C, amide group) $NS5A_{308–327}$ peptide was synthesized with the sequence $_{308}$ALPAWARPDYNPPLVESWRR$_{327}$. Core MOBKL1B (residues 33–216) and $NS5A_{308–327}$ peptide were mixed to a molar ratio ~1:1.2 protein/peptide at a final core MOBKL1B concentration of ~15 mg/ml. Crystals of core MOBKL1B–$NS5A_{308–327}$ complex were grown by hanging-drop vapor diffusion at 4°C. The reservoir solution was composed of 0.1 M HEPES, pH 7.5, 0.1 M potassium chloride and 15% (w/v) PEG5000. Crystals were cryoprotected by transfer to the reservoir solution with 20% (v/v) glycerol and frozen in liquid nitrogen.

Data collection and refinement

Data were collected at beam line X29 at the Brookhaven National Laboratory's National Synchrotron Light Source. The dataset was processed with DENZO, SCALEPACK and CCP (26, 27). Molecular replacement experiments were carried out with MOLREP and PHASER (CCP4 program suite). The structure of core MOBKL1B alone (PDB ID: 1PI1) (28) was used as a searching model in the initial molecular replacement experiment. Rigid body refinement and simulated annealing (29) were carried out sequentially. Model building was done with the O program (30). Non-crystallographic symmetry (NCS) restraints were applied to the two complexes in the asymmetric unit. No NCS was applied in the final round of refinement. Statistics are given in Table 2.

Results

311 **Identification of HCV NS5A interacting cellular proteins**

312 To identify HCV NS5A-interacting cellular proteins, we carried out a pull-down
313 assay in Huh-7.5 cells using Jc1 HCV, a fully infectious genotype 2a virus (17)
314 that expressed One-STrEP-tag (OST)-tagged NS5A (Jc1 NS5A-OST), followed
315 by liquid chromatography tandem mass spectrometry (LC-MS/MS). Two
316 independent analyses were performed using the same experimental conditions,
317 and nine cellular proteins with MASCOT scores higher than 100 were identified
318 (Table 1). The possible roles in virus replication of the identified host proteins
319 were further evaluated by siRNA knockdown. Except for the previously known
320 HCV replication factors CypA (11–14), phosphatidylinositol-4-kinase IIIα
321 (PIK4CA) (31) and newly identified MOBKL1B, siRNA knockdown of the other 6
322 NS5A-interacting host proteins did not affect HCV replication (not shown). We
323 therefore focused our attention on MOBKL1B, a component of the SWH tumor
324 suppressor pathway not previously implicated in HCV replication. To confirm the
325 interaction between MOBKL1B and NS5A, we performed yeast two-hybrid
326 interaction assays with MOBKL1B and each of the individual HCV proteins and
327 found that MOBKL1B bound to HCV NS5A, confirming the pull-down results (Fig.
328 1). Moreover, NS5A was the only HCV protein with which an interaction with
329 MOBKL1B was detected. Thus, we further characterized the MOBKL1B–NS5A
330 interaction and its possible role in HCV replication.
331
332 **RNA interference implicates MOBKL1B in HCV RNA replication**

Given the robust interaction between NS5A and MOBKL1B, we used a depletion strategy to investigate the importance of MOBKL1B for HCV growth in cell culture. We depleted the endogenous protein in Huh-7.5 cells using a pool of MOBKL1B-targeting siRNAs (Dharmacon Smart Pool) before infection with genotype 2 HCV Jc1. Measured 72 h post-infection, siRNA-treated cells had no detectable MOBKL1B, which was associated with a 10- to 20-fold reduction in viral progeny released into the medium compared to control cells treated with irrelevant siRNA (Fig. 2A). Since a defect following infection may represent a block to viral entry, RNA replication, or infectious particle production, we next investigated the stage of the viral life cycle impacted by MOBKL1B depletion. To test the importance of MOBKL1B for RNA replication, we used an Huh-7.5-derived cell line lacking the HCV entry factor, CD81 (32); this allowed detection of single-cycle replication without contributions from viral spread. These cells were treated with MOBKL1B-specific individual siRNA #1 or #2, and then transfected with *in vitro*-transcribed Jc1 RNA encoding a luciferase reporter (Jc1FLAG(p7-nsGluc2A)) (19). We observed that viral RNA replication, as assessed by luciferase expression, was decreased ~95% and ~65% in cells treated with MOBKL1B siRNA #1 and #2 respectively, as measured at 48 h post-transfection (Fig. 2B). These results indicate that treatment with siRNA targeting MOBKL1B affected the RNA replication step of the HCV life cycle. Since siRNA #1 more strongly reduced RNA replication and MOBKL1B expression than siRNA #2, we selected it for subsequent experiments to achieve efficient endogenous MOBKL1B knockdown.

We believed the HCV RNA replication phenotype observed under conditions of MOBKL1B silencing was unlikely to be due to off target effects since 1) three different siRNAs targeting MOBKL1B gave the same HCV replication phenotype (Smart pool and two individual siRNAs, Figs. 2A and 2B), 2) different levels of endogenous, presumably fully functional, MOBKL1B achieved by differing efficacy of two different siRNAs correlated with the efficacy of HCV RNA replication (Fig. 2B) and 3) we had strong evidence that MOBKL1B was capable of physically interacting with the HCV NS5A protein. We therefore proceeded to characterize the role of MOBKL1B in HCV replication in greater detail.

To investigate whether in addition to effects on RNA replication MOBKL1B might affect HCV entry, we utilized HIV-based luciferase-expressing pseudoparticles (HCVpp) expressing genotype 1a (H77) envelope proteins or G glycoprotein from vesicular stomatitis virus (VSV-G) as described (33). Knockdown of MOBKL1B did not affect the entry of HCV, suggesting that this host factor is not required for HCV entry (Fig. 2C). Next, we tested the importance of MOBKL1B for its effect on the replication of other HCV genotypes. Since authentic viral replication systems for most HCV genotypes are not yet available, we used infectious chimeric recombinant HCV variants bearing NS5A from genotypes 1–7 in a genotype 2 J6/JFH1 genome background (21). Although virus titers of some recombinant HCV variants were low, across all genotypes we observed a more than 5-fold reduction in infectious virus release into the medium after MOBKL1B knockdown in Huh-7.5 cells compared to irrelevant RNA

knockdown control (Fig. 2D). Taken altogether the data suggest that the host factor MOBKL1B positively influences the RNA replication of all HCV genotypes.

Mapping the Minimal MOBKL1B binding motif in NS5A

Given the likely role of MOBKL1B in HCV RNA replication and its interaction with NS5A, we set out to characterize the physical interaction in greater detail. Yeast two-hybrid assays had shown that NS5A was the only HCV protein that specifically bound MOBKL1B (Fig. 1). To identify the MOBKL1B binding motif on NS5A, we carried out further yeast two-hybrid analyses using serially deleted and alanine substitution mutants (Fig. 3A and 3B). Deletion of residues 314–322 or 323–337 reduced the MOBKL1B–NS5A interaction, and alanine substitution further pinpointed residues in the region of amino acids 315–324 in NS5A domain II as required for the interaction (Fig. 3A and 3B). To further map the minimal interaction sequence and to quantify the MOBKL1B–NS5A binding affinity, we performed biosensor assays using a series of serially deleted NS5A peptides (Fig. 3C). These experiments indicated that the minimal NS5A motif for MOBKL1B interaction (amino acids 310–327) bound with an apparent affinity of 18 ± 1 μM (mean ± s.d., K_d) (Fig. 3*C*, black curve). Interestingly, this binding motif is highly conserved in all seven HCV genotypes (Fig. 3D), consistent with the effect of MOBKL1B silencing on chimeric viruses containing NS5A from each of the seven genotypes (Fig. 2D).

Structure of the core MOBKL1B–NS5A$_{308–327}$ complex

To elucidate the molecular details of the MOBKL1B–NS5A interaction, we determined the co-crystal structure of protease-resistant core MOBKL1B (residues 33–216) (28) complexed with an NS5A peptide encompassing the MOBKL1B binding site (residues 308–327) at 1.95 Å resolution to an R_{free} of 0.225 (Rcryst = 0.196) (Fig. 4 and Table 2). The overall structure of core MOBKL1B in the complex is superimposable with that of the ligand-free protein. The structure showed two NS5A peptides binding to one MOBKL1B molecule (Fig. 4A). The peptide was resolved from L309 to E323 in one interaction (designated interaction 1) and from A308 to D316 in the other interaction (designated interaction 2). Interaction 1 is likely the relevant MOBKL1B–NS5A association detected *in vitro* based on the biosensor binding assay (Fig. 4B). The NS5A peptide (residues 305–316) encompassing interaction 2 showed no reliable binding to full-length MOBKL1B (Fig. 4B, green curve). In contrast, the structural properties of interaction 1 were consistent with the biochemical binding results (Fig. 3 and Fig. 4B) as described below.

The MOBKL1B–NS5A interaction consists of both hydrogen bonds and van der Waals surface contacts. NS5A residues W312 and Y317 are adjacent to each other in space, with the residues between them bulging out and covered by weak electron density (Fig. 4C). The side chain of W312 is embedded in a shallow hydrophobic depression formed by the well-conserved MOBKL1B residues, Y163, H164, F167, N180, L204 and L207. The W312 side chain is recognized by a hydrogen bond with the MOBKL1B Y163 main chain carbonyl oxygen (Fig. 4C). The hydroxyl oxygen of NS5A Y317 has bifurcated hydrogen-

bond interactions with the side chains of MOBKL1B E176 and N180. These intermolecular hydrogen bonds are likely secured by the MOBKL1B N180 side chain orientation through a hydrogen bond with MOBKL1B Y163 that exists in the absence of NS5A peptide (28) (Fig. 4C). These structural observations explain the severely impaired MOBKL1B–NS5A interaction caused by individual alanine substitutions of NS5A peptide residues W312 and Y317, for which no binding was detected (Fig. 4B). Similarly, full-length MOBKL1B did not bind to the $NS5A_{305–316}$ peptide, a region of NS5A found in the NS5A-MOBKL1B interaction 2. In contrast, we calculated that MOBKL1B bound to $NS5A_{308–327}$ peptide, a region found in NS5A-MOBKL1B interaction 1, with a Kd of 6.74 ± 1 μM (Fig. 4B).

In addition, residues P319 to V322 of NS5A contribute to the interaction by multiple van der Waals surface contacts and one hydrogen bond between the main-chain nitrogen atom of NS5A V322 and the side chain of MOBKL1B T181 (Fig. 4C). This explains the ~18-fold reduced binding affinity of the NS5A 310–320 peptide to the full-length MOBKL1B, compared to the NS5A 310–327 peptide (Fig. 3C). It is worth noting that the NS5A peptide contains internal stacking interactions through the W312 main-chain and a β-carbon atom, the Y317 side chain, the P319 residue and the N318 carbonyl group (Fig. 4C). Such stacking likely facilitates establishment of the interactions with MOBKL1B.

CypA-independent HCV unexpectedly reveals off-target replication inhibition mediated by MOBKL1B siRNA treatment

Similar to MOBKL1B, the host peptidyl-prolyl isomerase, CypA has been reported to interact with NS5A and is critically important for HCV RNA replication (11–14). Although its detailed function remains to be defined, NS5A mutations (D316E and Y317N, hereafter designated DEYN) that permit CypA-independent replication have been reported (13). Interestingly, these mutations are located within the NS5A motif required for MOBKL1B binding. Because of this, and since the NS5A Y317 residue is critical for MOBKL1B–NS5A interaction *in vitro* (Fig. 4B, blue curve), we wondered whether DEYN NS5A from the CypA-independent virus would interact with MOBKL1B. We therefore examined the interaction of NS5A and MOBKL1B in the context of HCV replication after transfection of Huh-7.5 cells with wild-type HCV (Jc1 NS5A-OST) or the CypA-independent mutant (Jc1 NS5A-OST DEYN) genomic RNA. After lysis, a co-precipitation experiment was performed using antibodies to the OST tag in NS5A. Consistent with the previous *in vitro* experiment, MOBKL1B was co-precipitated with wild-type NS5A. Precipitation of the DEYN mutant NS5A, however, failed to co-precipitate MOBKL1B (Fig. 5A), as expected given the loss of residue Y317 critical for the NS5A-MOBKL1B interaction.

Because there was no interaction between the DEYN mutant NS5A and MOBKL1B, we expected that replication of such a mutant virus would be independent of MOBKL1B and be unaffected by MOBKL1B depletion. To test this, we constructed a CypA-independent mutant luciferase reporter virus (Jc1FLAG(p7-nsGluc2A)DEYN) and tested the effect of MOBKL1B and CypA depletion (Fig. 5B) on virus replication (Fig. 5C). Wild-type Jc1FLAG(p7-

nsGluc2A) replication was inhibited by the depletion of either CypA (~40-fold reduction at 48 h post-transfection) or MOBKL1B (~20-fold reduction). As expected, Jc1FLAG(p7-nsGluc2A)DEYN replication was not affected by CypA depletion. In contrast, and quite unexpectedly, its replication was impaired ~15 fold after MOBKL1B depletion (Fig 5C). It was unanticipated that replication of this CypA-independent virus would be reduced in MOBKL1B siRNA-treated cells, given that its NS5A did not interact with MOBKL1B in protein pull-down assays. These results were discordant from our initial finding that MOBKL1B-NS5A interactions were associated with efficient virus replication, and led us to question whether MOBKL1B was implicated in virus replication indirectly and not via direct interaction with NS5A. As well, these findings caused us to re-examine our siRNA gene knockdown strategy and to explore whether off-target inhibitory effects might be blocking virus replication.

Seed-sequence matched siRNA controls do not deplete MOBKL1B

To re-investigate the importance of MOBKL1B for HCV growth in cell culture, we redesigned our siRNA approach using two previously used MOBKL1B-specific siRNAs (#1 and #2), and a new siRNA (#3) to deplete endogenous MOBKL1B (Fig. 6A). In addition, we included both irrelevant (IRR) and recently reported C911/C1012 negative control siRNAs (34) for each MOBKL1B-specific siRNA, to more carefully investigate if effects of silencing could be due to off-target effects of the siRNAs. C911/C1012 control siRNAs for 19-mer and 21-mer siRNAs, respectively, are 3-base internal mismatch controls

where bases 9–11 or 10–12 are switched to the complementary nucleotides of the target mRNA specific siRNA. Compared to the targeting siRNAs, such control siRNAs do not lead to degradation of the siRNA target mRNA and usually exert a much less pronounced knockdown effect. However, they retain the same seed sequences (bases 2–8 of the siRNA antisense and sense strands) and therefore have the potential to retain any seed-dependent off-target effects (34, 35).

Endogenous MOBKL1B was efficiently depleted in cells treated with three different MOBKL1B-specific siRNAs but not with IRR control or their corresponding C911/C1012 control siRNAs, as expected (Fig. 6A). As a control for cytotoxicity, we showed that transfection with all siRNAs did not affect cell viability (Fig. 6B).

Seed-sequence matched siRNA controls show that MOBKL1B is not required for HCV replication in Huh-7.5 cells

To re-test the effect of MOBKL1B on viral RNA replication and infectious particle production, we first transfected Jc1FLAG(p7-nsGluc2A) RNA into CD81 knockdown Huh-7.5 cells that had been treated with the siRNAs, and quantified luciferase expression in the supernatant (Fig. 6C). We observed that although viral RNA replication was decreased by ~90% in cells treated with siRNA #1, this was likely an off-target effect because its control (#1 C911) had a comparable effect (Fig. 6C), despite normal MOBKL1B protein expression (Fig. 6A). The results were similar, but to a lesser degree, for siRNA #2, wherein transfection of its control (#2 C1012) also reduced virus genome replication relative to the

irrelevant RNA control. In the absence of the seed-sequence matched controls for both siRNA #1 and #2, the resultant reduction in virus genome replication (Fig. 2B), was easily misinterpreted as being related to MOBKL1B depletion. In contrast, transfection of siRNA #3, which efficiently reduced MOBKL1B levels, and its control, which did not (#3 C911), both failed to affect HCV RNA replication, suggesting that MOBKL1B depletion via this siRNA veritably had no effect on virus genome replication (Fig. 6C). This result observed for siRNA #3 contrasts directly with results initially obtained with siRNAs #1 and #2 (Fig. 2B) where levels of virus replication correlated with MOBKL1B levels. Because the latter experiment includes a seed-sequence control matching the targeting siRNA, interpretation is simplified, and we conclude that HCV RNA replication is independent from MOBKL1B expression.

To be complete, we tested whether MOBKL1B knockdown affected infectious particle production. The supernatant from the siRNA #3-transfected cells in Fig. 6C was added to Huh-7.5 cells, and infection was quantified by luciferase detection. As shown in Fig. 6D, infectious particle production was decreased to about 70% in cells treated with siRNA #3 relative to irrelevant RNA. However, infectious particle production was even lower from cells treated with siRNA #3 C911 control, where MOBKL1B levels were unaffected and thus should not be expected to affect infectivity. Thus, although siRNA #3 legitimately had no effect on HCV RNA replication (Fig. 6C), its effect on the generation of infectious particles was most likely due to off-target effects, since similar results were obtained by its C911 matched control (Fig. 6D). Similarly, MOBKL1B

depletion in immune suppressed human fetal liver cells (36) using siRNA #3 did not affect HCV RNA replication or infectious particle production (data not shown). Taken together, these more stringent siRNA knockdown experiments showed that there is no functional requirement for the MOBKL1B-NS5A interaction in HCV genome replication in cell culture. Furthermore, they suggest that all siRNA experiments should be carried out with matched seed-sequence controls to differentiate false and true positive results (Fig. 2B vs. Fig. 6C, Fig. 6D).

Discussion

In this report, we identified MOBKL1B, a component of the SWH tumor suppressor pathway, as an HCV NS5A binding partner. On the basis of initial MOBKL1B siRNA knockdown experiments, we believed that the MOBKL1B-NS5A interaction was essential for HCV genome replication and committed significant time and resources to characterize the interaction. However, we ultimately found that this interpretation was incorrect, and that our original MOBKL1B siRNAs had off-target inhibitory effects on HCV RNA replication. Although we tested three MOBKL1B siRNAs, all had off-target effects on RNA replication or virion production. The use of many more siRNAs of different sequence targeting the same gene might have been one way to diminish false positive results (34). Compensatory expression of the target protein after siRNA treatment and the restoration of the phenotype is also a valuable method to verify that a phenotype is due to depletion of the factor under study. However, this method can potentially fail, due to multiple reasons, such as suboptimal protein

562 restoration, erroneous post-translational modifications or localization, incorrect
563 timing of competing silencing and restoration, and undefined effects on other
564 interacting proteins.

565 In fact, while we were able to restore MOBKL1B protein levels to near
566 endogenous levels in the presence of siRNA #1 using an siRNA-resistant
567 MOBKL1B construct, expecting to restore HCV RNA replication, we saw no
568 corresponding rescue of HCV replication (data not shown). As an additional
569 control, we studied the depletion and restoration of large tumor suppressor
570 protein (LATS1), a component of the SWH tumor suppressor pathway whose
571 expression depends on MOBKL1B (37). Indeed, MOBKL1B depletion resulted in
572 co-depletion of LATS1. However the restoration of MOBKL1B did not rescue
573 LATS1 expression to pre-MOBKL1B knockdown levels (data not shown). Thus,
574 at the time we reasoned that failure to restore HCV replication in the setting of
575 the rescue experiment might be because the MOBKL1B was unable to function
576 properly due to alterations in other pathway components, which had not yet been
577 properly restored during the time frame of the experiment. In retrospect, we, and
578 likely other investigators, were too quick to dismiss a failure to restore function
579 upon successful factor reconstitution.

580 The subcellular localization of MOBKL1B in the presence and absence of
581 HCV would have been an additional useful way to analyze the interaction
582 between NS5A and MOBKL1B. However, despite using various anti-MOBKL1B
583 antibodies, we had difficulty obtaining reliable MOBKL1B-specific signals in

584 immunofluorescence experiments (data not shown), precluding the use of this
585 approach.

586 Of all the methods to discern whether off-target effects are contributing to
587 a phenotype under study, we would like to note the efficacy of the C911 and
588 C1012 control siRNAs in distinguishing between true and false positive results
589 after siRNA treatment. Although siRNA is a potent molecular tool to study the
590 function of target genes and also a potential therapeutic tool for various diseases,
591 off-target effects of siRNA can lead to deceptive discoveries and hamper the
592 therapeutic usage of RNAi (38, 39). On the basis of our observations, we suggest
593 that C911 and C1012 matched control siRNAs should be adopted for RNA
594 knockdown experiments as a more stringent control than IRR or scrambled RNAi.
595 Collectively, these results have demonstrated that multiple approaches should be
596 used to define functional protein interactions. These could include but not be
597 limited to gene knockdowns consisting of diverse siRNAs with seed-sequence
598 matched controls, protein colocalization, and compensatory expression of the
599 siRNA target protein. Performed early on, they would reduce or eliminate the
600 need for further studies if the effect of gene knockdown is not verified.

601 Although MOBKL1B is not apparently required for HCV replication in cell
602 culture, the interaction with NS5A does occur, and we were able to characterize
603 the peptide complex structurally in what is, to our knowledge, the first reported
604 co-crystal structure involving NS5A and a cellular binding partner. NS5A is a
605 membrane-anchored phosphoprotein composed of three domains (I, II, and III)
606 separated by low-complexity sequences (40). Among the three domains, NS5A

607 domain I is highly conserved across all HCV genotypes with an N-terminal
608 amphipathic α-helix that is responsible for membrane association (41). NS5A
609 domain II is intrinsically unstructured, lacking discrete secondary structures (42)
610 and may be inherently flexible, allowing NS5A to interact with multiple biological
611 partners (43–45). Although the NS5A peptide in the complex structure is short, it
612 highlights the flexible nature of NS5A domain II (42). We found that the NS5A
613 peptide binds to MOBKL1B without forming α-helical or β-strand elements,
614 allowing discontinuous amino acid residues to contact the MOBKL1B surface.
615 These results bear on how the structural flexibility of NS5A domain II contributes
616 to the broad virus-host interactions needed for virus replication. This observation
617 is highlighted by our finding that MOBKL1B and a previously described HCV
618 replication factor, CypA, share overlapping NS5A-binding motifs.

619 In the core MOBKL1B–NS5A peptide complex structure, the peptide
620 contains three putative CypA substrate proline residues (P315, P319 & P320)
621 (13), each of which adopted only *trans* conformational amide bonds (P319 &
622 P320, Fig 4*C* black arrows; P315, not shown). Furthermore, P319 and P320
623 stabilize the MOBKL1B–NS5A interaction via van der Waals contacts and P319
624 participates in internal stacking. It is therefore conceivable that *cis* conformations
625 of peptidyl-prolyl bonds at these positions will inhibit MOBKL1B–NS5A binding.
626 The minimal MOBKL1B binding domain of NS5A adopts a loop shape in our co-
627 crystal structure, suggesting that MOBKL1B-NS5A interactions may restrain the
628 inherent flexibility of NS5A domain II to produce a transiently stable conformation.
629 Despite characterization of a structural interaction between NS5A and MOBKL1B,

its relevance to HCV genome and virus replication has not been demonstrated. However, the identification of MOBKL1B as an NS5A-binding protein may shed light on the pathogenesis of hepatitis C. To our knowledge, this is the first report showing the direct connection between a cancer-associated virus and the SWH tumor suppressor pathway. Previous studies have shown that the phosphorylated active form of MOBKL1B is frequently lost in human hepatocarcinoma and that interruption of the SWH tumor suppressor pathway in mice can promote liver tumors (46–48). It is worth noting that a MOBKL1B residue, T181 (49), important for the normal function of this pathway makes a hydrogen bond with the NS5A peptide. Taken together with previous reports, our findings suggest that the connection between MOBKL1B–NS5A binding, the SWH tumor suppressor pathway, and HCV-induced hepatocellular carcinoma should be further examined.

Acknowledgements

We thank the staff of the Rockefeller Proteomics Resource Center for peptide synthesis and mass spectrometry analyses, Jens Bukh (University of Copenhagen, Denmark) for kindly providing recombinant HCV variants, David G. Myszka (Biosensor Tools LLC, Salt Lake City, UT) for assistance with the biosensor analyses, and Mayla Hsu for editing. We also thank the staff of the Rockefeller Structural Biology Resource Center and the X29 beam line (National Synchrotron Light Source). Research reported in this publication was supported by the National Cancer Institute of the National Institutes of Health under Award Number R01CA057973 (C. M. R.). The content is solely the responsibility of the authors and does not necessarily represent the official views of the National Institutes of Health. Additional financial support was provided by the Greenberg Medical Research Institute and the Starr Foundation (to C. M. R). H. C. was supported in part by a Merck Postdoctoral Fellowship at the Rockefeller University.

References

1. **Liang TJ, Rehermann B, Seeff LB, Hoofnagle JH. 2000** Pathogenesis, natural history, treatment, and prevention of hepatitis C. Ann Intern Med **132:**296–305.
2. **Schinazi R, Halfon P, Marcellin P, Asselah T. 2014** HCV direct-acting antiviral agents: the best interferon-free combination. Liver Int **34**:69–78.
3. **Tellinghuisen TL, Rice CM. 2002** Interaction between hepatitis C virus proteins and host cell factors. Curr Opin Microbiol **5:**419–427.
4. **Pawlotsky JM. 2013** NS5A inhibitors in the treatment of hepatitis C. J Hepatol **59**:375–382.
5. **Blight KJ, Kolykhalov AA, Rice CM. 2000** Efficient initiation of HCV RNA replication in cell culture. Science **290:**1972–1974.
6. **Appel N, Zayas M, Miller S, Krijnse-Locker J, Schaller T, Friebe P, Kallis S, Engel U, Bartenschlager R. 2008** Essential role of domain III of nonstructural protein 5A for hepatitis C virus infectious particle assembly. PLoS Pathog **4:**e1000035.
7. **Tellinghuisen TL, Foss KL, Treadaway JC, Rice CM. 2008** Identification of residues required for RNA replication in domain II and III of the hepatitis C virus NS5A protein. J Virol **82:**1073–1083.
8. **Zhao B, Tumaneng K, Guan KL. 2011** The Hippo pathway in organ size control, tissue regeneration and stem cell self-renewal. Nat Cell Biol **13:**877–883.
9. **Zeng Q, Hong W. 2008** The emerging role of the hippo pathway in cell contact inhibition, organ size control, and cancer development in mammals. Cancer Cell **13:**188–192.
10. **Harvey K, Tapon N. 2007** The Salvador-Warts-Hippo pathway - an emerging tumour-suppressor network. Nat Rev Cancer **7:**182–191.

11. **Kaul A, Stauffer S, Berger C, Pertel T, Schmitt J, Kallis S, Zayas M, Lohmann V, Luban J, Bartenschlager R. 2009** Essential role of cyclophilin A for hepatitis C virus replication and virus production and possible link to polyprotein cleavage kinetics. PLoS Pathog **5:**e1000546.

12. **Hanoulle X, Badillo A, Wieruszeski JM, Verdegem D, Landrieu I, Bartenschlager R, Penin F, Lippens G. 2009** Hepatitis C virus NS5A protein is a substrate for the peptidyl-prolyl cis/trans isomerase activity of cyclophilins A and B. J Biol Chem **284:**13589–13601.

13. **Yang F, Robotham JM, Grise H, Frausto S, Madan V, Zayas M, Bartenschlager R, Robinson M, Greenstein AE, Nag A, Logan TM, Bienkiewicz E, Tang H. 2010** A major determinant of cyclophilin dependence and cyclosporine susceptibility of hepatitis C virus identified by a genetic approach. PLoS Pathog **6:**e1001118.

14. **Foster TL, Gallay P, Stonehouse NJ, Harris M. 2011** Cyclophilin A interacts with domain II of hepatitis C virus NS5A and stimulates RNA binding in an isomerase-dependent manner. J Virol **85:**7460–7464.

15. **Baugh JM, Garcia-Rivera JA, Gallay PA. 2013** Host-targeting agents in the treatment of hepatitis C: a beginning and an end? Antiviral Res **100**:555–561.

16. **Lindenbach BD, Evans MJ, Syder AJ, Wölk B, Tellinghuisen TL, Liu CC, Maruyama T, Hynes RO, Burton DR, McKeating JA, Rice CM. 2005** Complete replication of hepatitis C Virus in cell culture. Science **309:**623–626.

17. **Pietschmann T, Kaul A, Koutsoudakis G, Shavinskaya A, Kallis S, Steinmann E, Abid K, Negro F, Dreux M, Cosset FL, Bartenschlager R. 2006** Construction and characterization of infectious intragenotypic and intergenotypic hepatitis C virus chimeras. Proc Natl Acad Sci USA **103:**7408–7413.

714 18. **Schaller T, Appel N, Koutsoudakis G, Kallis S, Lohmann V,**
715 **Pietschmann T, Bartenschlager R. 2007** Analysis of hepatitis C virus
716 superinfection exclusion by using novel fluorochrome gene-tagged viral
717 genomes. J Virol **81:**4591–4603.

718 19. **Marukian S, Jones CT, Andrus L, Evans MJ, Ritola KD, Charles ED,**
719 **Rice CM, Dustin LB. 2008** Cell culture-produced hepatitis C virus does not
720 infect peripheral blood mononuclear cells. Hepatology **48:**1843–1850.

721 20. **Lindenbach BD, Evans MJ, Syder AJ, Wölk B, Tellinghuisen TL, Liu CC,**
722 **Maruyama T, Hynes RO, Burton DR, McKeating JA, Rice CM. 2005**
723 Complete replication of hepatitis C Virus in cell culture. Science **309:**623–
724 626.

725 21. **Scheel TKH, Gottwein JM, Mikkelsen LS, Jensen TB, Bukh J. 2011**
726 Recombinant HCV variants with NS5A from genotypes 1–7 have different
727 sensitivities to an NS5A inhibitor but not interferon-α. Gastroenterology
728 **140:**1032–1043.

729 22. **Langelier C, von Schwedler UK, Fisher RD, De Domenico I, White PL,**
730 **Hill CP, Kaplan J, Ward D, Sundquist WI. 2006** Human ESCRT-II complex
731 and its role in human immunodeficiency virus type 1 release. J Virol
732 **80:**9465–9480.

733 23. **Mossessova E, Lima CD. 2000** Ulp1-SUMO crystal structure and genetic
734 analysis reveal conserved interactions and a regulatory element essential
735 for cell growth in yeast. Mol Cell **5:**865–876.

736 24. **Johnsson B, Lofas S, Lindquist G. 1991** Immobilization of proteins to a
737 carboxymethyldextran-modified gold surface for biospecific interaction
738 analysis in surface plasmon resonance sensors. Anal Biochem **198:**268–
739 277.

740 25. **Myszka DG. 1999** Improving biosensor analysis. J Mol Recognit **12:**279–
741 284.

742 26. **Otwinowski Z, Minor W. 1997** Processing of x-ray diffraction data
743 collected in oscillation mode. Method Enzymol **276:**307–326.

744 27. **CCP4. 1994** The CCP4 suite: Programs for protein crystallography. Acta
745 Crystallogr D **50:**760–763.

746 28. **Stavridi ES, Harris KG, Huyen Y, Bothos J, Verwoerd PM, Stayrook SE,**
747 **Pavletich NP, Jeffrey PD, Luca FC. 2003** Crystal structure of a human
748 Mob1 protein: toward understanding Mob-regulated cell cycle pathways.
749 Structure **11:**1163–1170.

750 29. **Brünger AT, Adams PD, Clore GM, DeLano WL, Gros P, Grosse-**
751 **Kunstleve RW, Jiang JS, Kuszewski J, Nilges M, Pannu NS Read RJ,**
752 **Rice LM, Simonson T, Warren GL. 1998** Crystallography & NMR system:
753 A new software suite for macromolecular structure determination. Acta
754 Crystallogr D **54:**905–921.

755 30. **Jones TA, Zou JY, Cowan SW, Kjeldgaard M. 1991** Improved methods for
756 building protein models in electron density maps and the location of errors in
757 these models. Acta Crystallogr A **47(Pt 2):**110–119.

758 31. **Tai AW, Benita Y, Peng LF, Kim SS, Sakamoto N, Xavier RJ, Chung RT.**
759 **2009** A functional genomic screen identifies cellular cofactors of hepatitis C
760 virus replication. Cell Host Microbe **5:**298–307.

761 32. **Witteveldt J, Evans MJ, Bitzegelo J, Koutsoudakis G, Owsianka AM,**
762 **Angus AG, Keck ZY, Foung SK, Pietschmann T, Rice CM, Patel AH.**
763 **2009** CD81 is dispensable for hepatitis C virus cell-to cell transmission in
764 hepatoma cells. J Gene Virol **90:**48–58.

765 33. **Evans MJ, von Hahn T, Tscherne DM, Syder AJ, Panis M, Wölk B,**
766 **Hatziioannou T, McKeating JA, Bieniasz PD, Rice CM. 2007** Claudin-1 is
767 a hepatitis C virus co-receptor required for a late step in entry. Nature **446**:
768 801–805.

769 34. **Buehler E, Chen Y, Martin S. 2012** C911: A bench-level control for

sequence specific siRNA off-target effects. PLoS One **7:**e51942.

35. **Birmingham A, Anderson EM, Reynolds A, Ilsley-Tyree D, Leake D, Fedorov Y, Baskerville S, Maksimova E, Robinson K, Karpilow J, Marshall WS, Khvorova A. 2006** 3' UTR seed matches, but not overall identity, are associated with RNAi off-targets. Nat Methods **3:**199–204.

36. **Andrus L, Marukina S, Jones CT, Catanese MT, Sheahan TP, Schoggins JW, Barry WT, Dustin LB, Trehan K, Ploss A, Bhatia SN, Rice CM. 2011** Expression of paramyxovirus V proteins promotes replication and spread of hepatitis C virus in cultures of primary human fetal liver cells. Hepatology **54:**1901–1912

37. **Nishio M, Hamada K, Kawahara K, Sasaki M, Noguchi F, Chiba S, Mizuno K, Suzuki SO, Dong Y, Tokuda M, Morikawa T, Hikasa H, Eggenschwiler J, Yabuta N, Nojima H, Nakagawa K, Hata Y, Nishina H, Mimori K, Mori M, Sasaki T, Mak TW, Nakano t, Itami S, Suzuki A. 2012** Cancer susceptibility and embryonic lethality in Mob1a/1b double-mutant mice. J Clin Invest **122:**4505–4518.

38. **Mohr S, Bakal C, Perrimon N. 2010** Genomic screening with RNAi: results and challenges. Annu Rev Biochem **79:**37–64.

39. **Arbuthnot P, Carmona S, Ely A. 2005** Exploiting the RNA interference pathway to counter hepatitis B virus replication. Liver Int **25:**9–15.

40. **Tellinghuisen TL, Marcotrigiano J, Gorbalenya AE, Rice CM. 2004** The NS5A protein of hepatitis C virus is a zinc metalloprotein. J Biol Chem **279:**48576–48587.

41. **Brass V, Bieck E, Montserret R, Wölk B, Hellings JA, Blum HE, Penin F, Moradpour D. 2002** An amino-terminal amphipathic alpha-helix mediates membrane association of the hepatitis C virus nonstructural protein 5A. J Biol Chem **277:**8130–8139.

42. **Liang Y, Ye H, Kang CB, Yoon HS. 2007** Domain 2 of nonstructural protein

5A (NS5A) of hepatitis C virus is natively unfolded. Biochemistry **46:**11550–11558.

43. **Tan SL, Nakao H, Vijaysri S, Neddermann P, Jacobs BL, Mayer BJ, Katze MG. 1999** NS5A, a nonstructural protein of hepatitis C virus, binds growth factor receptor-bound protein 2 adaptor protein in a Src homology 3 domain/ligand-dependent manner and perturbs mitogenic signaling. Proc Natl Acad Sci USA **96:**5533-5538.

44. **Pflugheber J, Fredericksen B, Sumpter R Jr, Wang C, Ware F, Sodora DL, Gale M Jr. 2002** Regulation of PKR and IRF-1 during hepatitis C virus RNA replication. Proc Natl Acad Sci USA **99:**4650-4655.

45. **Shirota Y, Luo H, Qin W, Kaneko S, Yamashita T, Kobayashi K, Murakami S. 2002** Hepatitis C virus (HCV) NS5A binds RNA-dependent RNA polymerase (RdRP) NS5B and modulates RNA-dependent RNA polymerase activity. J Biol Chem **277:**11149–11155.

46. **Lu L, Li Y, Kim SM, Bossuyt W, Liu P, Qiu Q, Wang Y, Halder G, Finegold MJ, Lee JS, Johnson RL. 2010** Hippo signaling is a potent in vivo growth and tumor suppressor pathway in the mammalian liver. Proc Natl Acad Sci USA **107:**1437–1442.

47. **Song H, Mak KK, Topol L, Yun K, Hu J, Garrett L, Chen Y, Park O, Chang J, Simpson RM, Wang CY, Gao B, Jiang J, Yang Y. 2010** Mammalian Mst1 and Mst2 kinases play essential roles in organ size control and tumor suppression. Proc Natl Acad Sci USA **107:**1431–1436.

48. **Zhou D, Conrad C, Xia F, Park JS, Payer B, Yin Y, Lauwers GY, Thasier W, Lee JT, Avruch J, Bardeesy N. 2009** Mst1 and Mst2 maintain hepatocyte quiescence and suppress hepatocellular carcinoma development through inactivation of the Yap1 oncogene. Cancer Cell **16:**425–438.

49. **Hirabayashi S, Nakagawa K, Sumita K, Hidaka S, Kawai T, Ikeda M,**

826 **Kawata A, Ohno K, Hata Y. 2008** Threonine 74 of MOB1 is a putative key
827 phosphorylation site by MST2 to form the scaffold to activate nuclear Dbf2-
828 related kinase 1. Oncogene **21:**4281–4292.

829

830 **Figure Legends**

831 **Figure 1. MOBKL1B interacts with NS5A.**

832 Yeast two-hybrid analysis of the interaction between MOBKL1B and ten HCV
833 proteins. MOBKL1B-AD (GAL4 activation domain) fusion or a control AD
834 construct (Empty) were co-expressed with core, E1, E2, p7, NS2, NS3, NS4A,
835 NS4B, NS5A or NS5B-DBD (GAL4 DNA-binding domain) fusions, or control DBD
836 construct (Empty), and tested for positive yeast two-hybrid interactions under
837 selective nutritional conditions (lacking leucine, tryptophan, histidine, and
838 adenosine). Each viral protein was derived from the Jc1 sequence.

839

840 **Figure 2. Treatment with MOBKL1B siRNA inhibits HCV RNA replication.**

841 (*A*) HCV growth in culture is inhibited by MOBKL1B depletion. Huh-7.5 cells were
842 transfected twice with MOBKL1B-specific or irrelevant (IRR) siRNA at 24 h
843 intervals, and were infected with HCV Jc1 48 h after the second transfection.
844 Depletion of endogenous MOBKL1B protein was analyzed by Western blotting
845 (top panel); β actin levels are shown as a control. The results shown are
846 representative of three independent experiments.

847 (*B*) MOBKL1B depletion blocked viral RNA replication. Depletion of MOBKL1B in
848 CD81 knockdown Huh-7.5 cells was performed, as above. Two individual
849 MOBKL1B-specific siRNAs (#1 and #2) were used. Jc1FLAG(p7-nsGluc2A) RNA
850 was transfected 48 h after the second siRNA transfection. At each indicated time
851 point, released luciferase was measured to analyze viral RNA replication (mean
852 of *n* = 3; error bars, s.d.). RLU, relative light units.

(*C*) MOBKL1B knockdown does not affect the entry of pseudoparticles. After siRNA #1 treatment, Huh-7.5 cells were infected with luciferase reporter pseudoparticles 48 h after the second siRNA transfection. Luciferase was measured at 48 h after infection. Values are normalized to RLU measured in irrelevant siRNA treated cells (mean of n = 3; error bars, s.d.). VSV-G, vesicular stomatitis virus glycoprotein; H77-HCV, HCV strain H77 glycoproteins. RLU, relative light units.

(*D*) MOBKL1B is also required for the replication of J6/JFH1-based HCV NS5A recombinants. MOBKL1B depletion and viral genome transfection were performed as described above. Recombinant HCV variants were as follows: 1a, J6/JFH1(H77-NS5A); 1b, J6/JFH1(J4-NS5A)$_{R867H,\ C1185S}$; 2a, J6/JFH1(J6-NS5A)$_{F772S}$; 3a, J6/JFH1(S52-NS5A)$_{D1975G}$; 4a, J6/JFH1(ED43-NS5A)$_{F772S,\ Y1644H,\ E2267G}$; 5a, J6/JFH1(SA13-NS5A)$_{R1978G,\ S2416G}$; 6a, J6/JFH1(HK6a-NS5A)$_{I2268N}$; 7a, J6/JFH1(QC69-NS5A). The results shown are representative of two independent experiments. The dashed line indicates the quantitation limit of the assay.

Figure 3. Mapping the MOBKL1B binding site in NS5A.

(*A*) Yeast two-hybrid mapping of the MOBKL1B binding motif in NS5A. An MOBKL1B-AD fusion or a control AD construct (Empty) was co-expressed with serially deleted NS5A-DBD fusion or control DBD construct (Empty), and tested for positive yeast two-hybrid interactions under selective nutritional conditions (lacking leucine, tryptophan, histidine, and adenosine). NS5A deletion mutants were derived from genotype 1b, Con1. Numbers indicate the Con1 NS5A amino

acid positions.

(*B*) A schematic of NS5A is shown at the top panel. JFH1 NS5A amino acid positions are indicated. Yeast two-hybrid interactions are shown at the bottom panel. Numbers indicate the JFH1 NS5A amino acid positions. Note that JFH1 NS5A residues 310-335 are equivalent to Con1 NS5A residues 314–339.

(*C*) Biosensor binding isotherms for full length MOBKL1B binding to GST-JFH1 NS5A peptides. Triplicate data points are shown for each condition. Apparent binding affinities (K_ds) derived after fitting to simple one-to-one binding model were as follows: $NS5A_{310–335}$, 24 ± 1 μM; $NS5A_{310–327}$, 18 ± 1 μM; $NS5A_{310–324}$, 182 ± 39 μM; $NS5A_{310–320}$, 830 ± 100 μM; $NS5A_{314–329}$, no binding detected (means ± s.d.). Note that adaptive mutations in 1b, 2a, 3a, 4a, 5a and 6a recombinant HCV variants (Fig 2*D*), are not located in the NS5A MOBKL1B-binding motif.

(*D*) Sequence alignment of the MOBKL1B minimal binding motif of NS5A for the seven HCV genotypes. Asterisks indicate residues absolutely conserved in all genotypes. JFH1 NS5A amino acid positions are indicated.

Figure 4. Structure of core MOBKL1B–$NS5A_{308–327}$ complex.

(*A*) Core MOBKL1B (residues 33–216) with the $NS5A_{308–327}$ peptide depicted in ribbon representation as two views related by a 180° rotation. Nine α helices and two β strands are numbered as previously reported (28). There are two MOBKL1B–NS5A peptide interactions: interaction 1 and interaction 2, in which $NS5A_{308–327}$ peptide was determined from L309 to E323 in interaction 1, and from

899 A308 to D316 in interaction 2. H, α helix; S, β strand; N, N terminus; C, C
900 terminus.
901 (*B*) Biosensor binding isotherms for full-length MOBKL1B binding to GST-NS5A
902 peptides. Triplicate data points are shown for each condition. No binding was
903 detected for $NS5A_{308–327}$ W312A and Y317A or for $NS5A_{305–316}$ Wt in interaction 2.
904 (*C*) Close-up views of interaction 1. The NS5A peptide (stick) binding to the
905 shallow hydrophobic patch of MOBKL1B in space-filling models or ribbon
906 representation, left and right panel, respectively. Amino acid residues
907 participating in the MOBKL1B–NS5A interaction are highlighted by showing their
908 side chains and labeled with the corresponding amino acid sequence number.
909 Left panel, NS5A residues labeled in black. Right panel, MOBKL1B residues in
910 blue. Black arrows in left panel point out *trans* conformational amide bonds at
911 P319 and P320 NS5A residues that are putative CypA substrates.
912
913 **Figure 5. MOBKL1B depletion reduces CypA-independent HCV replication**
914 **despite lack of MOBKL1B-NS5A interaction.**
915 (*A*) NS5A bearing the DEYN mutation does not bind to MOBKL1B. One-STrEP-
916 tag (OST) fused NS5A was purified using Strep-Tactin Sepharose from Jc1
917 NS5A-OST wild-type- or DEYN mutant-transfected Huh-7.5 cell lysates. Left
918 panels, Western blot signals of MOBKL1B and NS5A in the input lysates using
919 anti-MOBKL1B and anti-NS5A antibodies. Right panels, Western blot signals
920 following affinity purification of NS5A.
921 (*B*) Depletion of endogenous CypA or MOBKL1B protein in CD81 knockdown

922 Huh-7.5 cells was analyzed by Western blotting; β actin is included as a control.
923 (*C*) Viral genome replication following CypA or MOBKL1B knockdown. At each
924 indicated time point, released luciferase was measured to analyze viral RNA
925 replication (mean of *n* = 3; error bars, s.d.). RLU, relative light units.
926
927 **Figure 6. Seed-sequence matched siRNA shows that MOBKL1B is not**
928 **required for HCV RNA replication in Huh-7.5 cells.**
929 (*A*) Three MOBKL1B-specific (#1, #2 & #3), their seed-sequence matched control
930 (#1 C911, #2 C1012 & #3 C911) siRNAs or irrelevant (IRR) siRNA were
931 transfected into Huh-7.5 cells as described for Figure 2. Depletion of endogenous
932 MOBKL1B protein was analyzed by Western blotting. β actin levels are shown as
933 a control.
934 (*B*) MOBKL1B siRNA treatment is not cytotoxic. Huh-7.5 cells were transfected
935 twice with three individual MOBKL1B-specific siRNAs (#1, #2 and #3), their seed-
936 sequence matched siRNAs (#1 C911, #2 C1012 and #3 C911) or irrelevant (IRR)
937 siRNA at 24 h intervals. Toxicity of the MOBKL1B knockdown was evaluated with
938 luminescent cell viability assay (mean of *n* = 3; error bars, s.d.). RLU, relative
939 light units.
940 (*C*) MOBKL1B depletion does not inhibit HCV genome replication. Depletion of
941 MOBKL1B in CD81 knockdown Huh-7.5 cells was performed, as above.
942 Jc1FLAG(p7-nsGluc2A) was transfected 48 h after the second siRNA
943 transfection. Media was collected 48 h later for luciferase quantitation. (D)
944 MOBKL1B depletion and infectious virus production. Naïve Huh-7.5 cells were

infected from the media from cells treated with IRR, siRNA #3 and siRNA #3 C911 (shown in C), and luciferase was measured to analyze infectious virus production. Values are normalized to RLU measured in irrelevant siRNA-treated cells (mean of *n* = 3; error bars, s.d.).

Table 1. Cellular proteins co-purified with HCV NS5A identified by LC-MS/MS analyses.

Protein name	Entrez Gene ID	Mass (Da)	MASCOT score[a]	No. of observed peptides[a]	Cellular localization
BIN1	274	64887	7490, 8165	371, 361	cytoplasm/ membrane/ nucleus
NAP1L1	4673	45631	2470, 2233	122, 115	cytoplasm/ nucleus
NAP1L4	4676	42968	1908, 1253	167, 167	cytoplasm/ nucleus
PPIA	5478	18229	1203, 894	75, 75	cytoplasm/ membrane
PIK4CA	5297	233595	412, 684	34, 48	membrane
AMPH	273	76381	405, 305	37, 24	cytoplasm/ membrane
MOBKL1B	55233	25246	285, 413	19, 15	cytoplasm
USP19	10869	153242	261, 391	20, 38	membrane
PDIA6	10130	48490	243, 111	11, 7	membrane

[a] Values represent the results of two independent analyses.

Table 2. Crystallographic data and refinement statistics

Complex	Core MOBKL1B–NS5A(x-y)
PDB ID	4J1V
Data collection	
Source	NSLS X29
Wavelength (Å)	1.075

Resolution (Å)	50-1.95 (1.97-1.95)
Space group	$P2_1$
Unit cell	
a, b, c (Å)	50.1, 54.5, 86.6
α, β, γ (˚)	90, 89.9, 90
Observations	120225
Unique reflections	34680
Redundancy	3.5 (3.0)
Completeness (%)	99.2 (97.4)
Mean I/σI	24.5
R-merge on I[a]	0.04 (0.08)
Cut-off criteria I/σI	0
Refinement statistics	
Resolution limits (Å)	50-1.95 (1.97-1.95)
Number of reflections	34083
Completeness (%)	99.5
Cut-off criteria I/σI	0
Number of atoms	
Protein	3146
Solvent	387
Rcryst[b]	0.196 (0.219)
R_{free} (5% of data)	0.225 (0.252)
Bonds (Å)/Angles (˚)[c]	0.0056/1.02
Mean B value (Å^2)	30.0
Ramachandran plot	
Most favored (%)	93.3
Additionally allowed (%)	6.7
Generously allowed (%)	0
Disallowed (%)	0

Numbers in parentheses indicate the range of the highest resolution bin and statistics for data in this resolution bin.

[a] $Rmerge = \sum hkl \sum i|I(hkl)i - \langle I(hkl)\rangle|/\sum hkl \sum i \langle I(hkl)i\rangle$.

[b] Rcryst $= \sum hkl\ |Fo(hkl)-Fc(hkl)|/\sum hkl\ |Fo(hkl)|$, where Fo and Fc are observed and calculated structure factors, respectively.

[c] Values indicate root-mean-square deviations in bond lengths and bond angles.

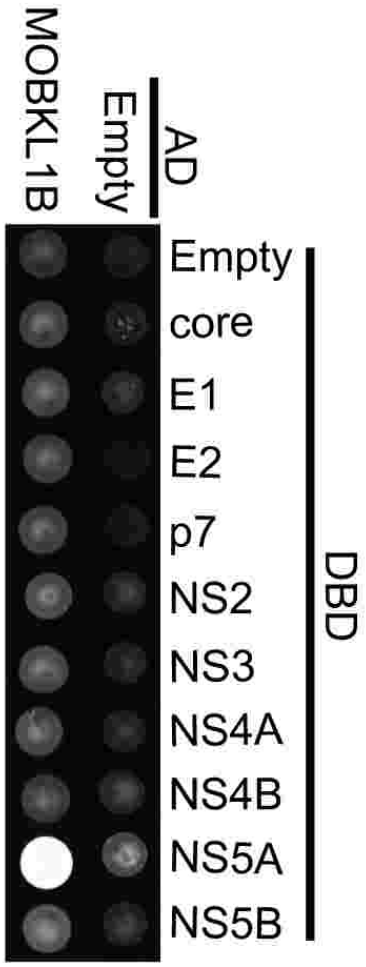

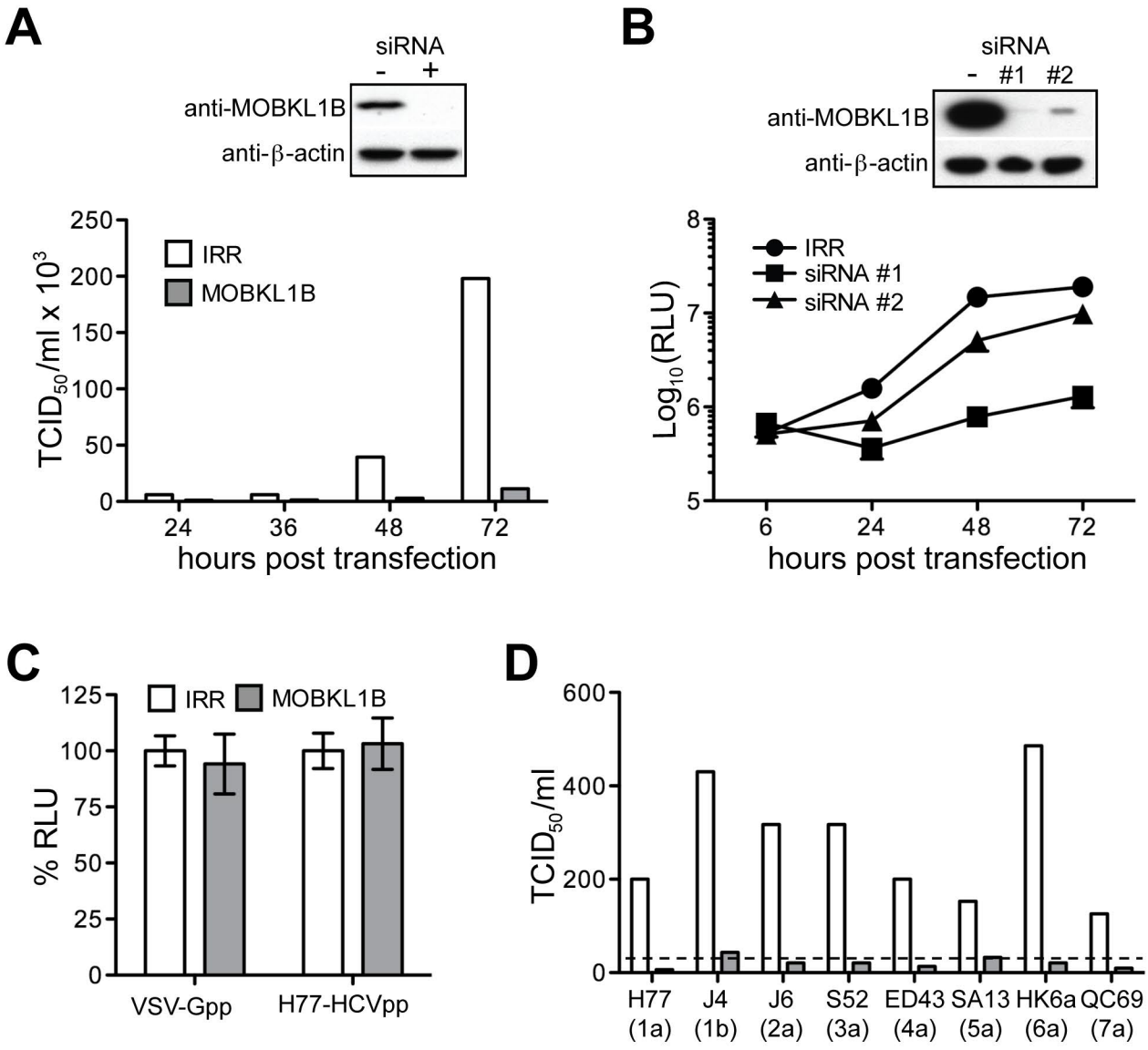

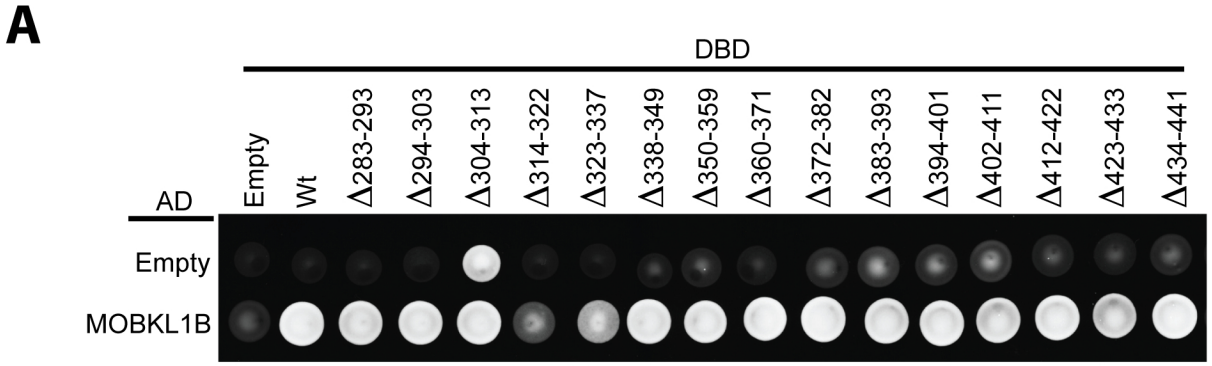

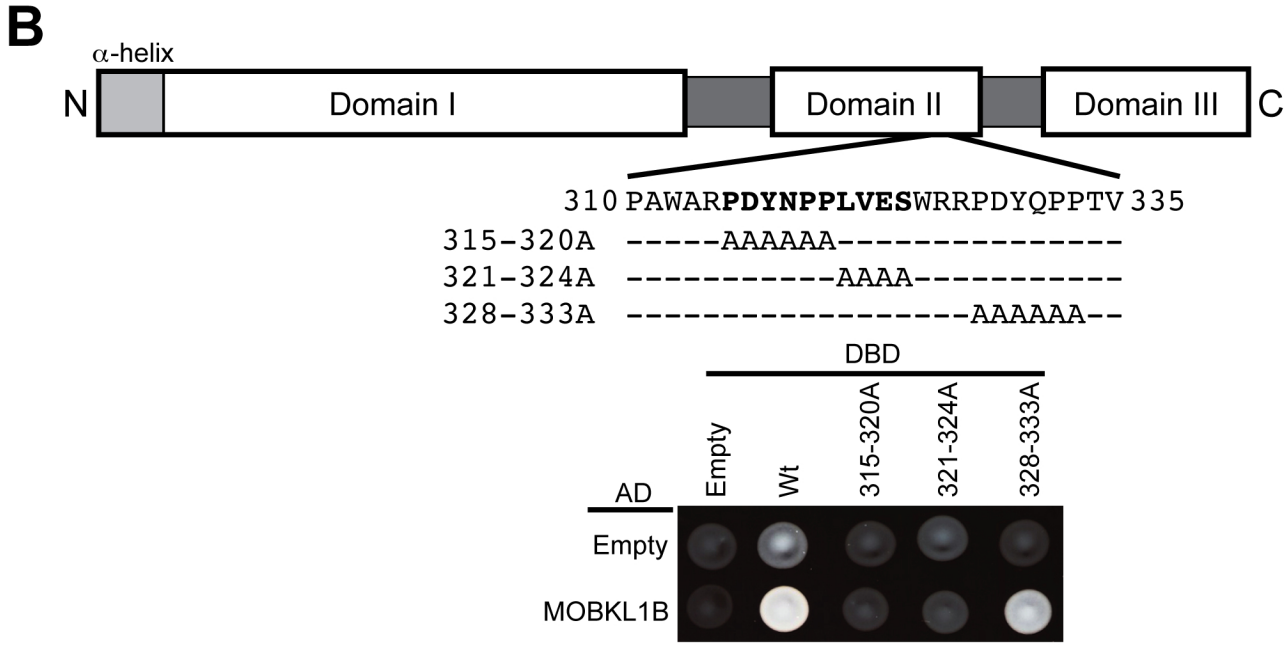

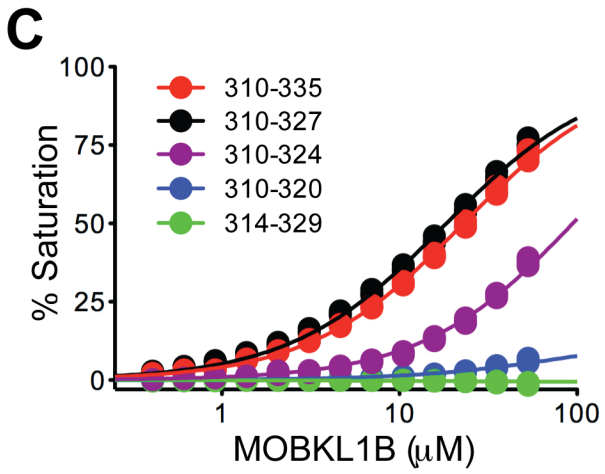

D

```
JFH-1(2a)     PAWARPDYNPPLVESWRR
H77(1a)       PVWARPDYNPPLVETWKK
Con1/J4(1b)   PIWARPDYNPPLLESWKD
J6 (2a)       PAWARPDYNPPLVESWKR
S52 (3a)      PIWARPDYNPPLLDRWKA
ED43 (4a)     PIWARPDYNPPLTETWKQ
SA13 (5a)     PIWARPGYDPPLLETWKQ
HK6a (6a)     PIWARPDYNPPLIQAWQM
QC69 (7a)     PIWARPDYNPPVVENWKD
              * **** * **    *
```